N,N′-Bisbenzylidenebenzene-1,4-diamines and *N,N′*-Bisbenzylidenenaphthalene-1,4-diamines as Sirtuin Type 2 (SIRT2) Inhibitors

Päivi H. Kiviranta,*[,†] Jukka Leppänen,[†] Sergiy Kyrylenko,[§] Heikki S. Salo,[†] Maija Lahtela-Kakkonen,[†] Anu J. Tervo,[†,#] Carsten Wittekindt,[†] Tiina Suuronen,[§] Erkki Kuusisto,[§] Tomi Järvinen,[†] Antero Salminen,[§,‡] Antti Poso,[†] and Erik A. A. Wallén[†]

Department of Pharmaceutical Chemistry and Department of Neuroscience and Neurology, University of Kuopio, P.O. Box 1627, 70211 Kuopio, Finland, and Department of Neurology, Kuopio University Hospital, P.O. Box 1777, 70211 Kuopio, Finland

Received May 12, 2006

A series of *N,N′*-bisbenzylidenebenzene-1,4-diamine and *N,N′*-bisbenzylidenenaphthalene-1,4-diamine derivatives were synthesized as inhibitors for human sirtuin type 2 (SIRT2). The design of the new compounds was based on two earlier reported hits from molecular modeling and virtual screening. The most potent compound was *N,N′*-bis(2-hydroxybenzylidene)benzene-1,4-diamine, which was equipotent with the most potent hit compound and well-known SIRT2 inhibitor sirtinol.

Introduction

Silent information regulator 2 (Sir2) protein is a nicotinamide adenine dinucleotide (NAD^+) dependent class III histone deacetylase (HDAC), which is found in prokaryotes and all eukaryotes.[1−3] Sir2 catalyzes the cleavage of the glycosidic bond between nicotinamide and ADP-ribose of NAD^+, followed by transfer of the acetyl group from an acetylated lysine residue to ADP-ribose, resulting in free nicotinamide and 2′- and 3′-*O*-acetyl-ADP-ribose.[1,4,5] Sir2 is required for several cellular functions, for example, chromatin silencing,[3] cell cycle, metabolism, and life span.[1,6,7] Seven human sirtuin type (SIRT) homologues are known so far.[1,8] SIRT2 is located principally in the cytoplasm of brain and muscle cells.[9] It has been shown to deacetylate lysine-40 of α-tubulin and colocalize with the cytoplasmic microtubules together with HDAC6.[10,11] The SIRT2 protein level increases during the mitotic exit in the cell cycle.[12] SIRT2 has also been reported to interact with the homeobox transcription factor HOXA10.[13] It has been postulated that SIRT2 inhibitors could be beneficial in patients suffering from neurodegenerative diseases and cancer.[14,15]

The NAD^+-dependent deacetylase activity is inhibited by the NAD^+ hydrolysis product nicotinamide. Besides nicotinamide, there are only a few known SIRT2 inhibitors. 8,9-Dihydroxybenzo[4,5]furo[3,2-*c*]chromen-6-one (A3) and 2-{[1-(2-hydroxynaphthalen-1-yl)meth-(*E*)-ylidene]amino}-*N*-(1-phenylethyl)benzamide (sirtinol) were the first reported potent SIRT2 inhibitors.[16] Recently 4-[(2-hydroxy-1-naphthalenylmethylene)amino]-*N*-(1-phenylethyl)benzamide (*para*-sirtinol)[17] and 6-chloro-2,3,4,9-tetrahydro-1*H*-carbazole-1-carboxylic acid amide (EX-527)[18] were also reported as SIRT2 inhibitors.

The crystal structure of SIRT2[19] was used as a starting point for molecular modeling and virtual screening. A search in the Maybridge database resulted in five compounds that showed inhibitory activity for SIRT2.[20] The IC_{50} values of the two most potent compounds 1,4-bis[2-(4-hydroxyphenyl)ethylamino]anthraquinone **1** (Maybridge JFD00244) and 5-(2-{[1-(3,5-dichloro-2-hydroxyphenyl)meth-(*E*)-ylidene]amino}phenylsulfanylmethyl)-4-hydroxymethyl-2-methylpyridin-3-ol **2** (Maybridge CD04097) were 56.7 and 74.3 μM, respectively (Figure 1).[20]

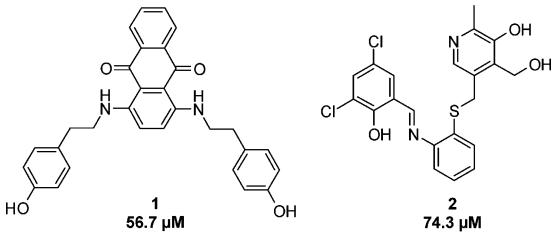

Figure 1. Two most potent compounds found by molecular modeling and virtual screening.[20]

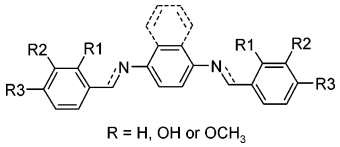

Figure 2. General structures of the new series of compounds.

The two compounds in Figure 1 have structural backbones that are new for SIRT2 inhibitors. The common structural features in the two compounds in Figure 1 are that both have a central aromatic group, which is disubstituted with two tethered hydroxy substituted aromatic groups. The phenolic hydroxyl groups of sirtinol and its analogues have been reported to be important for inhibitory activity.[16,17] The symmetrical **1** is 1,4-disubstituted. The length of the tether is three atoms, and the tether is connected via a nitrogen atom with an amine function. The unsymmetrical **2** is 1,2-disubstituted. The lengths of the tethers are two atoms, and the tethers are connected via a nitrogen atom with an imine function or via a sulfur atom with a sulfide function.

A new series of SIRT2 inhibitors with the general structure in Figure 2 was designed based on **1** and **2**. In the new series of compounds the central aromatic group is a 1,4-disubstituted benzene or naphthalene, the tether length is two atoms, it is connected via a nitrogen atom with an amine or an imine function, and the tethered aromatic group is a phenyl group. The choice of a naphthalene group as the central aromatic group was also supported by the fact that naphthalene derivatives have been reported to inhibit yeast Sir2 inhibitors.[21]

* To whom correspondence should be addressed. Phone: +358-17-163714. Fax: +358-17-162456. E-mail: paivi.kiviranta@uku.fi.
† Department of Pharmaceutical Chemistry, University of Kuopio.
§ Department of Neuroscience and Neurology, University of Kuopio.
# Current location: AstraZeneca R&D Mölndal, SC2, Pepparedsleden 1, 431 83 Mölndal, Sweden.
‡ Kuopio University Hospital.

10.1021/jm060566j CCC: $33.50
Published on Web 12/06/2006

Scheme 1. Synthetic Route for **3** and **4**[a]

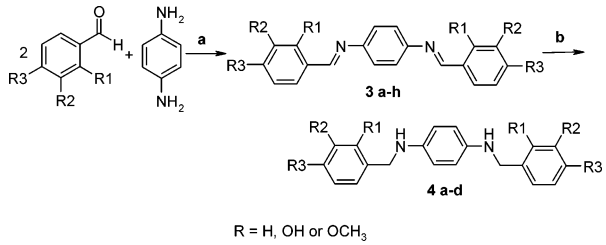

[a] Reagents: (a) EtOH; (b) $NaBH_4$, 1,2-dimethoxyethane.

Table 1. Structures of **3** and Their % Inhibition at 200 μM

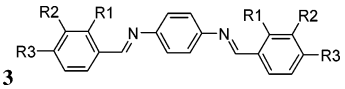

3

compd	R1	R2	R3	inhibition at 200 μM ± SD,[a] %
3a	H	H	H	35 ± 1.4
3b	OH	H	H	56 ± 8.2
3c	H	OH	H	12 ± 0.9
3d	H	H	OH	22 ± 1.6
3e	H	OH	OH	13 ± 0.2
3f	OCH_3	H	H	13 ± 0.5
3g	H	OCH_3	H	20 ± 1.2
3h	H	H	OCH_3	ND[b]

[a] SD = standard deviation. [b] The product did not dissolve.

Table 2. Structures of **4** and Their % Inhibition at 200 μM

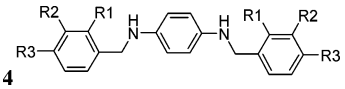

4

compd	R1	R2	R3	inhibition at 200 μM ± SD,[a] %
4a	H	H	H	21 ± 1.7
4b	OH	H	H	27 ± 2.4
4c	H	OH	H	8 ± 0.4
4d	H	H	OH	14 ± 0.5

[a] SD = standard deviation.

Chemistry

The compounds were synthesized via imine formation from benzene-1,4-diamine (or naphthalene-1,4-diamine) and the appropriate aldehyde (Scheme 1). The imine groups of the compounds from benzene-1,4-diamine were reduced with sodium borohydride.

Results and Discussion

The structures of the compounds and their inhibitory activities at 200 μM are presented in Tables 1−3. The IC_{50} values are presented for the most potent compounds in Table 4. The unsubstituted *N*,*N*′-bisbenzylidenebenzene-1,4-diamine (**3a**) gave an inhibition of 35% at 200 μM (Table 1). This shows that the new backbone is a moderate inhibitor of SIRT2, even when it is unsubstituted. *N*,*N*′-Bis(2-hydroxybenzylidene)benzene-1,4-diamine (**3b**) was the most potent inhibitor in the series with hydroxy substituted derivatives **3b**−**e**. Compound **3b** had an inhibition of 56% at 200 μM and an IC_{50} of 58.4 μM (Table 4). The methoxy substituted derivatives **3f**−**g** had lower inhibitory activities than the unsubstituted compound **3a**. The inhibitory activity of the para-substituted methoxy derivative **3h** was not determined because of an extremely low solubility.

The reduction of the imine function of **3a**−**d** resulted in **4a**−**d** (Table 2). Compounds **4a**−**d** are more flexible than **3a**−**d** because of deletion of the conjugated double bond between the aromatic rings. Compounds **4a**−**d** had a slightly lower inhibitory activity compared to compounds **3a**−**d**, the ortho-hydroxy substituted **4b** being again the most potent with an inhibition of 27% at 200 μM.

Table 3. Structures of **5** and Their % Inhibition at 200 μM

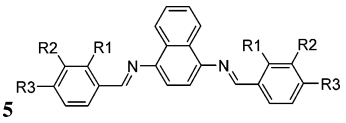

5

compd	R1	R2	R3	inhibition at 200 mM ± SD,[a] %
5a	H	H	H	18 ± 0.5
5b	OH	H	H	38 ± 1.2
5c	H	OH	H	53 ± 1.9
5d	H	H	OH	64 ± 1.9
5e	OCH_3	H	H	34 ± 1.2
5f	H	OCH_3	H	20 ± 0.2
5g	H	H	OCH_3	17 ± 1.1

[a] SD = standard deviation.

Table 4. IC_{50} Values of the Most Potent Compounds

compd	IC_{50} ± SD,[a] μmol/L
sirtinol	45.1 ± 1.6
1	56.7 ± 4.2
2	74.3 ± 1.5
3b	58.4 ± 14.8
5c	195.9 ± 10.9
5d	137.4 ± 8.8

[a] SD = standard deviation.

The unsubstituted *N*,*N*′-bisbenzylidenenaphthalene-1,4-diamine (**5a**) resulted in an inhibition of 18% at 200 μM (Table 3). This showed that the replacement of the central benzene group by a naphthalene group lowered the inhibitory activity slightly. However, all hydroxy substituted derivatives **5b**−**d** show improved inhibitory activities compared to the unsubstituted **5a**. Interestingly, the meta- and para-substituted **5c** and **5d** are the most potent compounds in this series with inhibitions of 53% and 64% at 200 μM, respectively, and IC_{50} of 195.9 and 137.4 μM, respectively. The methoxy substituted **5e**−**g** are equipotent with the unsubstituted **5a** but slightly less potent than the most potent hydroxy substituted **5c**−**d**.

When the compounds from Tables 1−3 are compared, it can be seen that the most potent compounds **3b**, **5c**, and **5d** have almost equal percentages of inhibition at 200 μM (56%, 53%, and 64%, respectively). Since these are only three compounds that have over 50% inhibition at 200 μM, their IC_{50} values were determined. In the in vitro assay for SIRT2 activity, poor solubility of several compounds was observed when determining the inhibition at higher concentrations. This was an additional reason not to determine the IC_{50} of compounds with less than 50% inhibition at 200 μM. The most potent compound **3b** has an IC_{50} of 58.4 μM, which is equipotent with the most potent hit compound **1** and sirtinol (Table 4). *N*,*N*′-Bis(3-hydroxybenzylidene)naphthalene-1,4-diamine (**5c**) and *N*,*N*′-bis(4-hydroxybenzylidene)naphthalene-1,4-diamine (**5d**) gave slightly higher IC_{50} values of 195.9 and 137.4 μM, respectively. The difference can be explained by the relatively large standard deviation of the percent inhibition of **3b** (56% ± 8.2%) at 200 μM. The Hill slopes of the inhibition curves did not deviate significantly from unity.

An interesting observation regarding the conformation of the compounds is that the most potent compound **3b** has hydroxyl groups in the ortho positions, which create strong intramolecular hydrogen bonds with the electronegative nitrogen atoms. The

hydrogen bonds have an effect on the NMR spectra of **3b**, giving a more downfield chemical shift of the hydroxyl groups (in DMSO-d_6). The same chemical shift cannot be observed for *N*,*N*′-bis(2-hydroxybenzyl)benzene-1,4-diamine (**4b**) but can again be observed for *N*,*N*′-bis(2-hydroxybenzylidene)naphthalene-1,4-diamine (**5b**).

To elucidate the binding possibilities of the SIRT2 inhibitors, compounds **3b**, **5c**, **5d**, sirtinol, **1**, and **2** were docked to the crystal structure of SIRT2.[22] Compounds **3b**, **5c**, and **5d** were able to adopt binding modes that shared similarities with the best ranked binding conformation of sirtinol. Compound **2** was also able to bind in the same area of the cavity. However, a similar binding pose for **1** could not be found in these dockings.

Conclusions

A series of *N*,*N*′-bisbenzylidenebenzene-1,4-diamine and *N*,*N*′-bisbenzylidenenaphthalene-1,4-diamine derivatives were synthesized and tested in vitro against SIRT2. The most potent compounds were **3b**, **5c**, and **5d** with IC_{50} of 58.4, 195.9, and 137.4 μM, respectively. Compound **3b** was equipotent with the well-known SIRT2 inhibitor sirtinol. These compounds have a new type of backbone for SIRT2 inhibitors. The new compounds were able to adopt binding modes that shared similarities with the best ranked binding conformation of sirtinol. The synthesized compounds are symmetrical, but there is no requirement of symmetry in the binding site of the SIRT2 inhibitor, and therefore, the next study will involve the synthesis of unsymmetrical compounds.

Experimental Section

General. NMR spectra (Bruker Avance 500, Bruker Biospin, Switzerland; 500.1 MHz for ^{1}H and 125.8 MHz for ^{13}C) were measured in DMSO-d_6 if not otherwise noted, and chemical shifts are expressed in ppm relative to tetramethylsilane as an internal standard. Positive ion mass spectra (ESI-MS) were acquired with a LCQ quadrupole ion trap mass spectrometer (Finnigan MAT, San Jose, CA) equipped with an electrospray ionization source. Combustion analyses for CHN were measured on Thermo Quest CE Instruments EA 1110 CHNS-O elemental analyzer. Flash chromatography was performed on silica gel. The reactions were performed in 1−7 mmol scale.

General Method for Synthesis of Imines 3a−h and 5a−g. The appropriate aldehyde (2.0−2.5 equiv) was added to a solution 1,4-phenylenediamine (1.0 equiv) in anhydrous ethanol (20 mL) or naphthalene-1,4-diamine (1.0 equiv) in anhydrous tetrahydrofuran (except **5c** in anhydrous acetonitrile) (20 mL). The reaction was performed under an argon or nitrogen atmosphere and protected from light. Benzene-1,4-diamine reactions were stirred at room temperature or refluxed if necessary. The product precipitated out of the reaction mixture. Naphthalene-1,4-diamine reactions were stirred overnight at room temperature. Afterward, the solvent was evaporated and the residue was washed with methanol.

***N*,*N*′-Bisbenzylidenebenzene-1,4-diamine (3a).** Benzaldehyde (2.1 equiv), room temperature for 1 h (77%). ^{1}H NMR: δ = 7.33 (s, 4 H), 7.48−7.51 (m, 6 H), 7.93−7.95 (m, 4 H), 8.63 (s, 2H). ^{13}C NMR: δ = 121.62, 128.39, 128.42, 131.00, 135.91, 149.16, 159.39. ESI-MS (*m*/*z*): 285 $[M + H]^+$. Anal. ($C_{20}H_{16}N_2$) C, H, N.

***N*,*N*′-Bis(2-hydroxybenzylidene)benzene-1,4-diamine (3b).** 2-Hydroxybenzaldehyde (2.0 equiv), reflux for 3.5 h (99%). The ^{1}H NMR parameters were solved precisely with the PERCHit iterator[23] using PERCH software.[24] ^{1}H NMR: δ = 6.977 (d, ^3J = 8.28 Hz, ^4J = 1.06 Hz, 2 H), 6.995 (t, ^3J = 7.70, 7.27 Hz, ^4J = 1.06 Hz, 2 H), 7.426 (td, ^3J = 8.28, 7.27 Hz, ^4J = 1.72 Hz, 2 H), 7.545 (s, 4 H), 7.673 (dd, ^3J = 7.70 Hz, ^4J = 1.72 Hz, 2 H), 9.030 (s, 2 H), 13.068 (s, 2 OH). ^{13}C NMR: δ = 116.51, 119.08, 119.27, 122.44, 132.47, 133.22, 146.58, 160.23, 163.05. ESI-MS (*m*/*z*): 317 $[M + H]^+$. Anal. ($C_{20}H_{16}N_2O_2$) C, H, N.

***N*,*N*′-Bis(3-hydroxybenzylidene)benzene-1,4-diamine (3c).** 3-Hydroxybenzaldehyde (2.0 equiv), room temperature for 3 days (80%). ^{1}H NMR: δ = 6.92−6.94 (m, 2 H), 7.30−7.38 (m, 10 H), 8.58 (s, 2 H), 9.66 (s, 2 OH). ^{13}C NMR: δ = 114.18, 118.62, 120.20, 121.88, 129.70, 137.39, 149.18, 157.62, 159.89. ESI-MS (*m*/*z*): 317 $[M + H]^+$. Anal. ($C_{20}H_{16}N_2O_2 \cdot 0.2H_2O$) C, H, N.

***N*,*N*′-Bis(4-hydroxybenzylidene)benzene-1,4-diamine (3d).** 4-Hydroxybenzaldehyde (2.0 equiv), reflux for 3.0 h (56%). ^{1}H NMR: δ = 6.89 (d, ^3J = 8.5 Hz, 4 H), 7.26 (s, 4 H), 7.78 (d, ^3J = 8.5 Hz, 4 H), 8.51 (s, 2 H), 10.08 (s, 2 OH). ^{13}C NMR: δ = 115.56, 121.66, 127.56, 130.50, 149.22, 158.98, 160.48. ESI-MS (*m*/*z*): 317 $[M + H]^+$. Anal. ($C_{20}H_{16}N_2O_2 \cdot 0.5H_2O$) C, H, N.

***N*,*N*′-Bis(3,4-dihydroxybenzylidene)benzene-1,4-diamine (3e).** 3,4-Dihydroxybenzaldehyde (2.1 equiv), room temperature overnight (63%). ^{1}H NMR (DMSO-d_6/CD_3OD): δ = 6.87 (d, ^3J = 8.1 Hz, 2 H), 7.21 (dd, ^3J = 8.1 Hz, ^4J = 1.8 Hz, 2 H), 7.25 (s, 4 H), 7.44−7.45 (m, 2 H), 8.42 (s, 2 H). ^{13}C NMR (DMSO-d_6/CD_3OD): δ = 114.33, 115.63, 121.94, 122.88, 128.50, 145.76, 149.34, 149.56, 159.51. ESI-MS (*m*/*z*): 349 $[M + H]^+$. Anal. ($C_{20}H_{16}N_2O_4 \cdot 0.3H_2O$) C, H, N.

***N*,*N*′-Bis(2-methoxybenzylidene)benzene-1,4-diamine (3f).** 2-Methoxybenzaldehyde (2.0 equiv), room temperature for 2 h (95%). ^{1}H NMR: δ = 3.92 (s, 6 H), 7.03−7.06 (m, 2 H), 7.08−7.10 (m, 2 H), 7.26 (s, 4 H), 7.46−7.50 (m, 2 H), 8.06−8.08 (m, 2 H), 8.92 (s, 2 H). ^{13}C NMR: δ = 55.57, 111.53, 120.51, 121.73, 124.12, 126.86, 132.78, 149.93, 154.75, 159.23. ESI-MS (*m*/*z*): 345 $[M + H]^+$. Anal. ($C_{22}H_{20}N_2O_2 \cdot 0.1H_2O$) C, H, N.

***N*,*N*′-Bis(3-methoxybenzylidene)benzene-1,4-diamine (3g).** 3-Methoxybenzaldehyde (2.5 equiv), reflux 2 h (65%). ^{1}H NMR: δ = 3.84 (s, 6H), 7.10−7.12 (m, 2 H), 7.36 (s, 4 H), 7.43−7.46 (m, 2 H), 7.52−7.53 (m, 4 H), 8.66 (s, 2 H). ^{13}C NMR: δ = 55.14, 112.48, 117.58, 121.54, 121.94, 129.80, 137.47, 149.16, 159.49, 159.82. ESI-MS (*m*/*z*): 345 $[M + H]^+$. Anal. ($C_{22}H_{20}N_2O_2 \cdot 0.1H_2O$) C, H, N.

***N*,*N*′-Bis(4-methoxybenzylidene)benzene-1,4-diamine (3h).** 4-Methoxybenzaldehyde (3.7 equiv), room temperature for 3 h (97%). ^{1}H NMR: δ = 3.89 (s, 6 H), 7.00 (d, ^3J = 8.5 Hz, 4 H), 7.25 (s, 4 H), 7.86 (d, ^3J = 8.5 Hz, 4 H), 8.47 (s, 2 H). ^{13}C NMR: δ = 55.69, 114.72, 122.32, 129.97, 130.92, 150.20, 159.32, 162.70. ESI-MS (*m*/*z*): 345 $[M + H]^+$. Anal. ($C_{22}H_{20}N_2O_2 \cdot 0.1H_2O$) C, H, N.

***N*,*N*′-Bisbenzylidenenaphthalene-1,4-diamine (5a).** Benzaldehyde (2.1 equiv), room temperature overnight (64%). ^{1}H NMR: δ = 7.31 (s, 2 H), 7.57−7.62 (m, 8 H), 8.08−8.10 (m, 4 H), 8.37−8.39 (m, 2 H), 8.76 (s, 2 H). ^{13}C NMR: δ = 113.18, 123.45, 126.21, 128.76, 128.76, 128.92, 131.42, 136.21, 146.18, 159.97. ESI-MS (*m*/*z*): 335 $[M + H]^+$. Anal. ($C_{24}H_{18}N_2 \cdot 0.2H_2O$) C, H, N.

***N*,*N*′-Bis(2-hydroxybenzylidene)naphthalene-1,4-diamine (5b).** 2-Hydroxybenzaldehyde (2.1 equiv), room temperature overnight (51%). ^{1}H NMR: δ = 7.03−7.06 (m, 4 H), 7.46−7.50 (s, 2 H), 7.55 (s, 2 H), 7.70−7.72 (m, 2 H), 7.77−7.79 (m, 2 H), 8.25−8.27 (m, 2 H), 9.07 (s, 2 H), 13.06 (s, 2 OH). ^{13}C NMR: δ = 114.73, 116.57, 119.24, 119.73, 122.79, 127.14, 128.23, 132.37, 133.47, 144.16, 160.22, 163.46. ESI-MS (*m*/*z*): 367 $[M + H]^+$. Anal. ($C_{24}H_{18}N_2O_2$) C, H, N.

***N*,*N*′-Bis(3-hydroxybenzylidene)naphthalene-1,4-diamine (5c).** 3-Hydroxybenzaldehyde (2.5 equiv), room temperature for 2.5 h (27%). ^{1}H NMR: δ = 6.98−6.99 (m, 2 H), 7.26−7.62 (m, 10 H), 8.36 (m, 2 H), 8.68 (s, 2 H), 9.76 (s, 2 OH). ^{13}C NMR: δ =113.32, 114.41, 118.87, 120.46, 123.48, 126.30, 128.96, 129.90, 137.62, 146.16, 157.79, 160.15. ESI-MS (*m*/*z*): 367 $[M + H]^+$. Anal. ($C_{24}H_{18}N_2O_2 \cdot 1.1H_2O$) C, H, N.

***N*,*N*′-Bis(4-hydroxybenzylidene)naphthalene-1,4-diamine (5d).** 4-Hydroxybenzaldehyde (2.1 equiv), room temperature for 3 days (47%). ^{1}H NMR: δ = 6.94 (d, ^3J = 8.2 Hz, 4 H), 7.21 (s, 2 H), 7.56−7.58 (m, 2 H), 7.92 (d, ^3J = 8.2 Hz, 4 H), 8.35−8.37 (m, 2 H), 8.60 (s, 2 H), 10.16 (s, 2 OH). ^{13}C NMR: δ = 113.10, 115.74, 123.57, 126.03, 127.87, 129.08, 130.83, 146.23, 159.25, 160.72. ESI-MS (*m*/*z*): 367 $[M + H]^+$. Anal. ($C_{24}H_{18}N_2O_2 \cdot 1.7CH_3OH$) C, H, N. CH_3OH was observed in the NMR spectra.

***N,N′*-Bis(2-methoxybenzylidene)naphthalene-1,4-diamine (5e).** 2-Methoxybenzaldehyde (2.0 equiv), room temperature overnight (18%). ^{1}H NMR: δ = 3.93 (s, 6 H), 7.12−7.15 (m, 2 H), 7.19−7.21 (m, 4 H), 7.55−7.60 (m, 4 H), 8.23−8.25 (m, 2 H), 8.33−8.35 (m, 2 H), 9.00 (s, 2 H). ^{13}C NMR: δ = 55.74, 111.98, 113.20, 120.70, 123.45, 124.07, 126.19, 127.10, 128.88, 133.16, 146.79, 154.85, 159.25. ESI-MS (*m*/*z*): 395 $[M + H]^+$. Anal. ($C_{26}H_{22}N_2O_2 \cdot 0.1H_2O$) C, H, N.

***N,N′*-Bis(3-methoxybenzylidene)naphthalene-1,4-diamine (5f).** 3-Methoxybenzaldehyde (2.4 equiv), room temperature for 2 days (60%). ^{1}H NMR ($CDCl_3$): δ = 3.92 (s, 6 H), 7.07−7.09 (m, 4 H), 7.40−7.44 (m, 2 H), 7.52−7.53 (m, 2 H), 7.56−7.58 (m, 2 H), 7.67−7.67 (m, 2 H), 8.38−8.40 (m, 2 H), 8.56 (s, 2 H). ^{13}C NMR ($CDCl_3$): δ = 55.46, 112.17, 112.84, 118.16, 122.40, 123.86, 126.30, 129.27, 129.78, 137.92, 147.27, 159.52, 160.05. ESI-MS (*m*/*z*): 395 $[M + H]^+$. Anal. ($C_{26}H_{22}N_2O_2 \cdot 0.3H_2O$) C, H, N.

***N,N′*-Bis(4-methoxybenzylidene)naphthalene-1,4-diamine (5g).** 4-Methoxybenzaldehyde (2.0 equiv), room temperature for 2 days (66%). ^{1}H NMR: δ = 3.89 (s, 6 H), 7.07 (d, ^3J = 8.4 Hz, 4 H), 7.19 (s, 2 H), 7.54−7.56 (m, 2 H), 8.00 (d, ^3J = 8.4 Hz, 4 H), 8.36−8.38 (m, 2 H), 8.62 (s, 2 H). ^{13}C NMR: δ = 55.30, 112.86, 114.16, 123.58, 125.90, 129.11, 129.27, 130.50, 146.37, 158.72, 161.99. ESI-MS (*m*/*z*): 395 $[M + H]^+$. Anal. ($C_{26}H_{22}N_2O_2 \cdot 0.1H_2O$) C, H, N.

General Method for Reduction of Imines for Amines. $NaBH_4$ (2.8−3.6 equiv) was added carefully in small portions to a solution of **3** (1.0 equiv) in 1,2-dimethoxyethane. After the mixture was stirred at room temperature for 1.5 h to 3 days, a catalytic amount of glacial acetic acid was added according to Krebs and Jørgensen.[25] The mixture was stirred at room temperature overnight. The solution was acidified to pH 1−2 using concentrated HCl and stirred for another 10 min. Then the solution was brought to pH 7 using a 2 M NaOH.[26] The mixture was diluted with water and extracted with CH_2Cl_2. The organic layer was washed once with water, dried over Na_2SO_4, and evaporated. The product was purified by flash chromatography.

***N,N′*-Bisbenzylbenzene-1,4-diamine (4a). 3a** and $NaBH_4$ (2.8 equiv), 2 h (43%). ^{1}H NMR: δ = 4.13 (d, ^3J = 5.3 Hz, 4 H), 5.31 (t, ^3J = 5.3 Hz, 2 NH), 6.40 (s, 4 H), 7.17−7.20 (m, 2 H), 7.26−7.29 (m, 4 H), 7.32−7.33 (m, 4 H). ^{13}C NMR: δ = 47.68, 113.71, 126.30, 127.15, 128.01, 140.03, 140.85. ESI-MS (*m*/*z*): 289 $[M + H]^+$. Anal. ($C_{20}H_{20}N_2 \cdot 0.1H_2O$) C, H, N.

***N,N′*-Bis(2-hydroxybenzyl)benzene-1,4-diamine (4b). 3b** and $NaBH_4$ (2.8 equiv), 1.5 h (30%). ^{1}H NMR: δ = 4.08 (s, 4 H), 5.18 (s, 2 NH), 6.44 (s, 4 H), 6.69−6.72 (m, 2 H), 6.76−6.78 (m, 2 H), 6.99−7.03 (m, 2 H), 7.17−7.18 (m, 2 H), 9.47 (s, 2 OH). ^{13}C NMR: δ = 43.10, 114.00, 114.70, 118.59, 126.01, 127.20, 128.28, 140.15, 155.03. ESI-MS (*m*/*z*): 321 $[M + H]^+$. Anal. ($C_{20}H_{20}N_2O_2 \cdot 0.3H_2O$) C, H, N.

***N,N′*-Bis(3-hydroxybenzyl)benzene-1,4-diamine (4c). 3c** and $NaBH_4$ (2.8 equiv), 3 days (36%). ^{1}H NMR: δ = 4.04−4.05 (m, 4 H), 5.26 (s, 2 NH), 6.38 (s, 4 H), 6.57−6.58 (m, 2 H), 6.73−6.74 (m, 4 H), 7.04−7.07 (m, 2 H), 9.18−9.20 (m, 2 OH). ^{13}C NMR: δ = 47.70, 113.32, 113.67, 113.93, 117.73, 128.97, 140.10, 142.46, 157.29. ESI-MS (*m*/*z*): 321 $[M + H]^+$. Anal. ($C_{20}H_{20}N_2O_2 \cdot 0.1H_2O$) C, H, N.

***N,N′*-Bis(4-hydroxybenzyl)benzene-1,4-diamine (4d). 3d** and $NaBH_4$ (3.6 equiv), 3 h (71%). ^{1}H NMR (D_2O): δ = 4.04 (s, 4 H), 6.60 (d, ^3J = 8.4 Hz, 4 H), 6.80 (s, 4H), 7.12 (d, ^3J = 8.4 Hz, 4 H). ^{13}C NMR (D_2O): δ = 51.97, 119.97, 121.52, 127.67, 132.58, 144.12, 168.03. ESI-MS (*m*/*z*): 321 $[M + H]^+$. Anal. ($C_{20}H_{16}N_2O_2 \cdot 2.2H_2O$) C, H, N.

In Vitro Assay for SIRT2 Activity. The inhibitory activities were determined using a radioactively labeled acetylated α-tubulin peptide as substrate. The α-tubulin peptide was labeled with [^{3}H]sodium acetate using benzotriazol-1-yloxytris(dimethylamino)-phosphonium hexafluorophosphate (BOP) reagent and purified by chromatography. The SIRT2 deacetylation reaction was performed in 100 μL of 1× HDAC buffer (Upstate Biotechnology), pH 8.0, and 500 μM NAD^+ (Sigma) with 40 000 counts per minute [^{3}H]peptide and 1 μg of recombinant GST-SIRT2 at 37 °C overnight. Addition of 50 μL of quenching solution, which was acidic, was used to stop the reaction. The released [^{3}H]acetylated product was extracted with ethyl acetate and counted by a liquid scintillation counter. Each experiment was repeated at least three times.

Docking Procedures. The docking studies were performed with the Gold molecular docking program, version 3.0,[27] and AutoDock software package, version 3.0.5,[28] using the crystal structure of SIRT2[22] (PDB entry 1J8F) as the target protein. The scoring of the dockings was based on the scoring functions implemented in the programs. In the Gold runs the GoldScore scoring function was used. The search area in the docking runs was limited to include the cavity that forms the active site of the protein and parts of the so-called hydrophobic pocket adjacent to the active site region. Both docking programs were able to produce congruent results and dock the compounds in the area of the active site cavity where the deacetylation reaction has been shown to take place. There is a narrow channel leading from the active site to the other side of the protein. This channel has been shown to be very hydrophilic and attract water molecules.[20] GRID[29] calculations showed that water molecules interact more favorably in that channel than the docked compounds. Therefore, docking results where the ligand was docked into the water channel were excluded from the analysis.

Acknowledgment. We thank Prof. Jouko Vepsäläinen for guidance in NMR, Jarkko Venäläinen, Ph.D., for his help with the in vitro data, and Tiina Koivunen for her skillful technical assistance, and we thank the Graduate School of Drug Discovery, the National Technology Agency of Finland, the Academy of Finland (Grant No. 108649 to E.A.A.W., Grant No. 106313 to J.L., and Grant No. 111453 to A.P.), and Association of Finnish Chemical Societies for financial support.

Supporting Information Available: Detailed experimental procedures for the syntheses, NMR spectra, ESI-MS results, and elemental analysis data for the new compounds, in vitro assay for SIRT2 activity, and the docking procedure. This material is available free of charge via the Internet at http://pubs.acs.org.

References

(1) Sauve, A. A.; Wolberger, C.; Schramm, V. L.; Boeke, J. D. The biochemistry of sirtuins. *Annu. Rev. Biochem.* **2006**, *75*, 435−465.
(2) Smith, J. S.; Brachmann, C. B.; Celic, I.; Kenna, M. A.; Muhammad, S.; Starai, V. J.; Avalos, J. L.; Escalante-Semerena, J. C.; Grubmeyer, C.; Wolberger, C.; Boeke, J. D. A phylogenetically conserved NAD^+-dependent protein deacetylase activity in the Sir2 protein family. *Proc. Natl. Acad. Sci. U.S.A.* **2000**, *97*, 6658−6663.
(3) Brachmann, C. B.; Sherman, J. M.; Devine, S. E.; Cameron, E. E.; Pillus, L.; Boeke, J. D. The SIR2 gene family, conserved from bacteria to humans, functions in silencing, cell cycle progression, and chromosome stability. *Genes Dev.* **1995**, *9*, 2888−2902.
(4) Tanner, K. G.; Landry, J.; Sternglanz, R.; Denu, J. M. Silent information regulator 2 family of NAD-dependent histone/protein deacetylases generates a unique product, 1-*O*-acetyl-ADP-ribose. *Proc. Natl. Acad. Sci. U.S.A.* **2000**, *97*, 14178−14182.
(5) Smith, B. C.; Denu, J. M. Sir2 protein deacetylases: evidence for chemical intermediates and functions of a conserved histidine. *Biochemistry* **2006**, *45*, 272−282.
(6) Guarente, L. Sir2 links chromatin silencing, metabolism, and aging. *Genes Dev.* **2000**, *14*, 1021−1026.
(7) Lin, S. J.; Ford, E.; Haigis, M.; Liszt, G.; Guarente, L. Calorie restriction extends yeast life span by lowering the level of NADH. *Genes Dev.* **2004**, *18*, 12−16.
(8) Frye, R. A. Phylogenetic classification of prokaryotic and eukaryotic Sir2-like proteins. *Biochem. Biophys. Res. Commun.* **2000**, *273*, 793−798.
(9) Afshar, G.; Murnane, J. P. Characterization of a human gene with sequence homology to *Saccharomyces cerevisiae* SIR2. *Gene* **1999**, *234*, 161−168.
(10) North, B. J.; Marshall, B. L.; Borra, M. T.; Denu, J. M.; Verdin, E. The human Sir2 ortholog, SIRT2, is an NAD^+-dependent tubulin deacetylase. *Mol. Cell* **2003**, *11*, 437−444.
(11) Hubbert, C.; Guardiola, A.; Shao, R.; Kawaguchi, Y.; Ito, A.; Nixon, A.; Yoshida, M.; Wang, X. F.; Yao, T. P. HDAC6 is a microtubule-associated deacetylase. *Nature* **2002**, *417*, 455−458.

(12) Dryden, S. C.; Nahhas, F. A.; Nowak, J. E.; Goustin, A. S.; Tainsky, M. A. Role for human SIRT2 NAD-dependent deacetylase activity in control of mitotic exit in the cell cycle. *Mol. Cell. Biol.* **2003**, *23*, 3173−3185.
(13) Bae, N. S.; Swanson, M. J.; Vassilev, A.; Howard, B. H. Human histone deacetylase SIRT2 interacts with the homeobox transcription factor HOXA10. *J. Biochem. (Tokyo)* **2004**, *135*, 695−700.
(14) Grubisha, O.; Rafty, L. A.; Takanishi, C. L.; Xu, X.; Tong, L.; Perraud, A. L.; Scharenberg, A. M.; Denu, J. M. Metabolite of SIR2 reaction modulates TRPM2 ion channel. *J. Biol. Chem.* **2006**, *281*, 14057−14065.
(15) Heltweg, B.; Gatbonton, T.; Schuler, A. D.; Posakony, J.; Li, H.; Goehle, S.; Kollipara, R.; DePinho, R. A.; Gu, Y.; Simon, J. A.; Bedalov, A. Antitumor activity of a small-molecule inhibitor of human silent information regulator 2 enzymes. *Cancer Res.* **2006**, *66*, 4368−4377.
(16) Grozinger, C. M.; Chao, E. D.; Blackwell, H. E.; Moazed, D.; Schreiber, S. L. Identification of a class of small molecule inhibitors of the sirtuin family of NAD-dependent deacetylases by phenotypic screening. *J. Biol. Chem.* **2001**, *276*, 38837−38843.
(17) Mai, A.; Massa, S.; Lavu, S.; Pezzi, R.; Simeoni, S.; Ragno, R.; Mariotti, F. R.; Chiani, F.; Camilloni, G.; Sinclair, D. A. Design, synthesis, and biological evaluation of sirtinol analogues as class III histone/protein deacetylase (sirtuin) inhibitors. *J. Med. Chem.* **2005**, *48*, 7789−7795.
(18) Napper, A. D.; Hixon, J.; McDonagh, T.; Keavey, K.; Pons, J. F.; Barker, J.; Yau, W. T.; Amouzegh, P.; Flegg, A.; Hamelin, E.; Thomas, R. J.; Kates, M.; Jones, S.; Navia, M. A.; Saunders, J. O.; DiStefano, P. S.; Curtis, R. Discovery of indoles as potent and selective inhibitors of the deacetylase SIRT1. *J. Med. Chem.* **2005**, *48*, 8045−8054.
(19) Finnin, M. S.; Donigian, J. R.; Pavletich, N. P. Structure of the histone deacetylase SIRT2. *Nat. Struct. Biol.* **2001**, *8*, 621−625.
(20) Tervo, A. J.; Kyrylenko, S.; Niskanen, P.; Salminen, A.; Leppanen, J.; Nyronen, T. H.; Jarvinen, T.; Poso, A. An in silico approach to discovering novel inhibitors of human sirtuin type 2. *J. Med. Chem.* **2004**, *47*, 6292−6298.
(21) Posakony, J.; Hirao, M.; Stevens, S.; Simon, J. A.; Bedalov, A. Inhibitors of Sir2: evaluation of splitomicin analogues. *J. Med. Chem.* **2004**, *47*, 2635−2644.
(22) Finnin, M. S.; Donigian, J. R.; Pavletich, N. P. Structure of the histone deacetylase SIRT2. *Nat. Struct. Biol.* **2001**, *8*, 621−625.
(23) Laatikainen, R.; Niemitz, M.; Weber, U.; Sundelin, J.; Hassinen, T.; Vepsäläinen, J. General strategies for total-lineshape-type spectral analysis of NMR spectra using integral-transform iterator. *J. Magn. Reson. A* **1996**, *120*, 1−10.
(24) *PERCH*, version 2004.1; PERCH Solutions Ltd.: Kuopio, Finland, 2004.
(25) Krebs, F. C.; Jorgensen, M. Synthesis and structural characterization of new stiff rod oligomeric domains by X-ray crystallography and NMR. *J. Org. Chem.* **2002**, *67*, 7511−7518.
(26) Lubben, M.; Feringa, B. A new method for the synthesis of nonsymmetric dinucleating ligands by aminomethylation of phenols and salicylaldehydes. *J. Org. Chem.* **1994**, *59*, 2227−2233.
(27) Jones, G.; Willett, P.; Glen, R. C.; Leach, A. R.; Taylor, R. Development and validation of a genetic algorithm for flexible docking. *J. Mol. Biol.* **1997**, *267*, 727−748.
(28) Morris, G. M.; Goodsell, D. S.; Halliday, R. S.; Huey, R.; Hart, W. E.; Belew, R. K.; Olson, A. J. Automated docking using a Lamarckian genetic algorithm and an empirical binding free energy function. *J. Comput. Chem.* **1998**, *19*, 1639−1662.
(29) Goodford, P. J. A computational procedure for determining energetically favorable binding sites on biologically important macromolecules. *J. Med. Chem.* **1985**, *28*, 849−857.

JM060566J